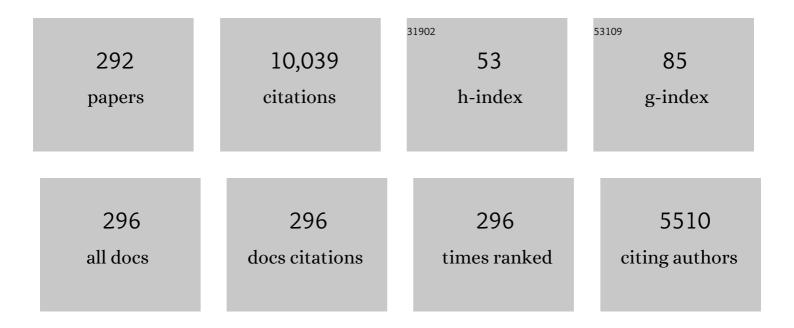
Chong Soo Lee

List of Publications by Year in descending order

Source: https://exaly.com/author-pdf/8213361/publications.pdf Version: 2024-02-01



#	Article	IF	CITATIONS
1	Role of {10–12} twinning characteristics in the deformation behavior of a polycrystalline magnesium alloy. Acta Materialia, 2010, 58, 5873-5885.	3.8	680
2	Stacking fault energy and plastic deformation of fully austenitic high manganese steels: Effect of Al addition. Materials Science & Engineering A: Structural Materials: Properties, Microstructure and Processing, 2010, 527, 3651-3661.	2.6	283
3	Ultrafine grained ferrite–martensite dual phase steels fabricated via equal channel angular pressing: Microstructure and tensile properties. Acta Materialia, 2005, 53, 3125-3134.	3.8	272
4	An analysis of the strain hardening behavior of ultra-fine grain pure titanium. Scripta Materialia, 2006, 54, 1785-1789.	2.6	196
5	Work hardening associated with É≻martensitic transformation, deformation twinning and dynamic strain aging in Fe–17Mn–0.6C and Fe–17Mn–0.8C TWIP steels. Materials Science & Engineering A: Structural Materials: Properties, Microstructure and Processing, 2011, 528, 7310-7316.	2.6	185
6	Activation mode dependent {10â^'12} twinning characteristics in a polycrystalline magnesium alloy. Scripta Materialia, 2010, 62, 202-205.	2.6	166
7	Hydrogen Delayed Fracture Properties and Internal Hydrogen Behavior of a Fe–18Mn–1.5Al–0.6C TWIP Steel. ISIJ International, 2009, 49, 1952-1959.	0.6	163
8	Enhanced osteoblast response to an equal channel angular pressing-processed pure titanium substrate with microrough surface topography. Acta Biomaterialia, 2009, 5, 3272-3280.	4.1	138
9	Microstructural influences on hydrogen delayed fracture of high strength steels. Materials Science & Engineering A: Structural Materials: Properties, Microstructure and Processing, 2009, 505, 105-110.	2.6	136
10	Effect of deformation on hydrogen trapping and effusion in TRIP-assisted steel. Acta Materialia, 2012, 60, 4085-4092.	3.8	126
11	Strain path dependence of {10â^'12} twinning activity in a polycrystalline magnesium alloy. Scripta Materialia, 2011, 64, 145-148.	2.6	117
12	Ultrahigh high-strain-rate superplasticity in a nanostructured high-entropy alloy. Nature Communications, 2020, 11, 2736.	5.8	116
13	Microstructural analysis on boundary sliding and its accommodation mode during superplastic deformation of Ti–6Al–4V alloy. Materials Science & Engineering A: Structural Materials: Properties, Microstructure and Processing, 1999, 263, 272-280.	2.6	112
14	Delayed static failure of twinning-induced plasticity steels. Scripta Materialia, 2012, 66, 960-965.	2.6	110
15	Effect of anisotropy on the low-cycle fatigue behavior of rolled AZ31 magnesium alloy. Materials Science & Engineering A: Structural Materials: Properties, Microstructure and Processing, 2010, 527, 417-423.	2.6	108
16	On the transitions of deformation modes of fully austenitic steels at room temperature. Metals and Materials International, 2010, 16, 1-6.	1.8	104
17	Enhanced superplasticity utilizing dynamic globularization of Ti–6Al–4V alloy. Materials Science & Engineering A: Structural Materials: Properties, Microstructure and Processing, 2008, 496, 150-158.	2.6	103
18	Low-cycle fatigue characteristics of rolled Mg–3Al–1Zn alloy. International Journal of Fatigue, 2010, 32, 1835-1842.	2.8	103

#	Article	IF	CITATIONS
19	In-plane anisotropic deformation behavior of rolled Mg–3Al–1Zn alloy by initial {10–12} twins. Materials Science & Engineering A: Structural Materials: Properties, Microstructure and Processing, 2013, 570, 149-163.	2.6	101
20	Enhanced stretch formability of rolled Mg–3Al–1Zn alloy at room temperature by initial {10–12} twins. Materials Science & Engineering A: Structural Materials: Properties, Microstructure and Processing, 2013, 578, 271-276.	2.6	100
21	Constitutive analysis of the high-temperature deformation of Ti–6Al–4V with a transformed microstructure. Acta Materialia, 2003, 51, 5613-5626.	3.8	99
22	Development of Ti and Mo micro-alloyed hot-rolled high strength sheet steel by controlling thermomechanical controlled processing schedule. Materials Science & Engineering A: Structural Materials: Properties, Microstructure and Processing, 2013, 565, 430-438.	2.6	98
23	Laser, tungsten inert gas, and metal active gas welding of DP780 steel: Comparison of hardness, tensile properties and fatigue resistance. Materials & Design, 2014, 64, 559-565.	5.1	98
24	The mechanism of enhanced resistance to the hydrogen delayed fracture in Al-added Fe–18Mn–0.6C twinning-induced plasticity steels. International Journal of Hydrogen Energy, 2012, 37, 9925-9932.	3.8	96
25	Role of É› martensite in tensile properties and hydrogen degradation of high-Mn steels. Materials Science & Engineering A: Structural Materials: Properties, Microstructure and Processing, 2012, 533, 87-95.	2.6	94
26	Low-temperature superplasticity of ultra-fine-grained Ti-6Al-4V processed by equal-channel angular pressing. Metallurgical and Materials Transactions A: Physical Metallurgy and Materials Science, 2006, 37, 381-391.	1.1	93
27	Prediction of flow stress in Ti–6Al–4V alloy with an equiaxed α+β microstructure by artificial neural networks. Materials Science & Engineering A: Structural Materials: Properties, Microstructure and Processing, 2008, 492, 276-282.	2.6	93
28	Effects of equal channel angular pressing temperature on deformation structures of pure Ti. Materials Science & Engineering A: Structural Materials: Properties, Microstructure and Processing, 2003, 342, 302-310.	2.6	91
29	Effects of rolling temperature on the microstructure and mechanical properties of Ti–Mo microalloyed hot-rolled high strength steel. Materials Science & Engineering A: Structural Materials: Properties, Microstructure and Processing, 2014, 605, 244-252.	2.6	89
30	Surface Modification of Multipass Caliber-Rolled Ti Alloy with Dexamethasone-Loaded Graphene for Dental Applications. ACS Applied Materials & amp; Interfaces, 2015, 7, 9598-9607.	4.0	82
31	Osteoconductivity of hydrophilic microstructured titanium implants with phosphate ion chemistry. Acta Biomaterialia, 2009, 5, 2311-2321.	4.1	81
32	Effects of temperature and initial microstructure on the equal channel angular pressing of Ti–6Al–4V alloy. Scripta Materialia, 2003, 48, 197-202.	2.6	77
33	Dissolution kinetics of delta ferrite in AISI 304 stainless steel produced by strip casting process. Materials Science & Engineering A: Structural Materials: Properties, Microstructure and Processing, 2003, 356, 390-398.	2.6	77
34	Multiple twinning modes in rolled Mg–3Al–1Zn alloy and their selection mechanism. Materials Science & Engineering A: Structural Materials: Properties, Microstructure and Processing, 2012, 532, 401-406.	2.6	76
35	Anisotropic yielding behavior of rolling textured high purity titanium. Materials Science & Engineering A: Structural Materials: Properties, Microstructure and Processing, 2015, 637, 215-221.	2.6	73
36	Deformation anisotropy and associated mechanisms in rolling textured high purity titanium. Journal of Alloys and Compounds, 2015, 651, 245-254.	2.8	73

#	Article	IF	CITATIONS
37	Flow softening behavior during high temperature deformation of AZ31Mg alloy. Journal of Materials Processing Technology, 2007, 187-188, 766-769.	3.1	71
38	Effects of vanadium carbides on hydrogen embrittlement of tempered martensitic steel. Metals and Materials International, 2016, 22, 364-372.	1.8	71
39	Finite-element analysis of microstructure evolution in the cogging of an Alloy 718 ingot. Materials Science & Engineering A: Structural Materials: Properties, Microstructure and Processing, 2007, 449-451, 722-726.	2.6	70
40	Effects of microstructural factors on quasi-static and dynamic deformation behaviors of Ti-6Al-4V alloys with widmanstÃ t ten structures. Metallurgical and Materials Transactions A: Physical Metallurgy and Materials Science, 2003, 34, 2541-2548.	1.1	69
41	Tensile deformation behavior of Fe–Mn–C TWIP steel with ultrafine elongated grain structure. Materials Letters, 2012, 75, 169-171.	1.3	69
42	Quantitative analysis on boundary sliding and its accommodation mode during superplastic deformation of two-phase Ti-6Al-4V alloy. Metallurgical and Materials Transactions A: Physical Metallurgy and Materials Science, 1998, 29, 217-226.	1.1	68
43	Effect of aluminium on hydrogen-induced fracture behaviour in austenitic Fe–Mn–C steel. Proceedings of the Royal Society A: Mathematical, Physical and Engineering Sciences, 2013, 469, 20120458.	1.0	66
44	Role of initial {10â^12} twin in the fatigue behavior of rolled Mg–3Al–1Zn alloy. Scripta Materialia, 2010, 62, 666-669.	2.6	64
45	Space-holder effect on designing pore structure and determining mechanical properties in porous titanium. Materials & Design, 2014, 57, 712-718.	5.1	64
46	Evaluation of bone healing with eggshellâ€derived bone graft substitutes in rat calvaria: A pilot study. Journal of Biomedical Materials Research - Part A, 2008, 87A, 203-214.	2.1	63
47	Enhancing the fatigue property of rolled AZ31 magnesium alloy by controlling {10-12} twinning-detwinning characteristics. Journal of Materials Research, 2010, 25, 784-792.	1.2	61
48	Grain refinement effect on cryogenic tensile ductility in a Fe–Mn–C twinning-induced plasticity steel. Materials & Design, 2013, 49, 234-241.	5.1	61
49	Effect of grain boundary engineering on hydrogen embrittlement in Fe-Mn-C TWIP steel at various strain rates. Corrosion Science, 2018, 142, 213-221.	3.0	61
50	Enhancing tensile properties of ultrafine-grained medium-carbon steel utilizing fine carbides. Materials Science & Engineering A: Structural Materials: Properties, Microstructure and Processing, 2011, 528, 6558-6564.	2.6	59
51	Mechanisms and Kinetics of Static Spheroidization of Hot-Worked Ti-6Al-2Sn-4Zr-2Mo-0.1Si with a Lamellar Microstructure. Metallurgical and Materials Transactions A: Physical Metallurgy and Materials Science, 2012, 43, 977-985.	1.1	59
52	Dynamic recrystallization behavior and microstructural evolution of Mg alloy AZ31 through high-speed rolling. Journal of Materials Science and Technology, 2018, 34, 1747-1755.	5.6	59
53	A study on diffusion bonding of superplastic Ti–6Al–4V ELI grade. Journal of Materials Processing Technology, 2007, 187-188, 526-529.	3.1	56
54	Dynamic deformation behavior and ballistic impact properties of Ti-6Al-4V alloy having equiaxed and bimodal microstructures. Metallurgical and Materials Transactions A: Physical Metallurgy and Materials Science, 2004, 35, 3103-3112.	1.1	55

#	Article	IF	CITATIONS
55	Ring-rolling design for a large-scale ring product of Ti–6Al–4V alloy. Journal of Materials Processing Technology, 2007, 187-188, 747-751.	3.1	55
56	Effects of alloy additions and tempering temperature on the sag resistance of Si–Cr spring steels. Materials Science & Engineering A: Structural Materials: Properties, Microstructure and Processing, 2000, 289, 8-17.	2.6	53
57	Energy-based approach to predict the fatigue life behavior of pre-strained Fe–18Mn TWIP steel. Materials Science & Engineering A: Structural Materials: Properties, Microstructure and Processing, 2011, 528, 4696-4702.	2.6	51
58	Caliber-rolled TWIP steel for high-strength wire rods with enhanced hydrogen-delayed fracture resistance. Scripta Materialia, 2012, 67, 681-684.	2.6	50
59	Quasi-static and dynamic deformation behavior of Ti–6Al–4V alloy containing fine α2-Ti3Al precipitates. Materials Science & Engineering A: Structural Materials: Properties, Microstructure and Processing, 2004, 366, 25-37.	2.6	48
60	Effects of tungsten on the hydrogen embrittlement behaviour of microalloyed steels. Corrosion Science, 2014, 82, 380-391.	3.0	48
61	Anisotropy in twinning characteristics and texture evolution of rolling textured high purity alpha phase titanium. Journal of Alloys and Compounds, 2016, 683, 92-99.	2.8	47
62	Ultrahigh-strength CoCrFeMnNi high-entropy alloy wire rod with excellent resistance to hydrogen embrittlement. Materials Science & Engineering A: Structural Materials: Properties, Microstructure and Processing, 2018, 732, 105-111.	2.6	47
63	Effects of microstructural morphology on quasi-static and dynamic deformation behavior of Ti-6Al-4V alloy. Metallurgical and Materials Transactions A: Physical Metallurgy and Materials Science, 2001, 32, 315-324.	1.1	46
64	Enhancement of high strain rate superplastic elongation of a modified 5154 Al by subsequent rolling after equal channel angular pressing. Scripta Materialia, 2004, 51, 479-483.	2.6	46
65	Effect of thermo hydrogen treatment on lattice defects and microstructure refinement of Ti6Al4V alloy. International Journal of Hydrogen Energy, 2010, 35, 6448-6454.	3.8	46
66	Shear band formation during hot compression of AZ31 Mg alloy sheets. Materials Science & Engineering A: Structural Materials: Properties, Microstructure and Processing, 2012, 558, 431-438.	2.6	46
67	Microstructure tailoring to enhance strength and ductility in Ti–13Nb–13Zr for biomedical applications. Scripta Materialia, 2013, 69, 785-788.	2.6	45
68	Role of Cu on hydrogen embrittlement behavior inÂFe–Mn–C–Cu TWIP steel. International Journal of Hydrogen Energy, 2015, 40, 7409-7419.	3.8	45
69	Artificial neural network modeling on the relative importance of alloying elements and heat treatment temperature to the stability of α and β phase in titanium alloys. Computational Materials Science, 2015, 107, 175-183.	1.4	45
70	Microstructural influence on low-temperature superplasticity of ultrafine-grained Ti–6Al–4V alloy. Materials Science & Engineering A: Structural Materials: Properties, Microstructure and Processing, 2005, 410-411, 156-159.	2.6	44
71	Microstructure and tensile behavior of Al and Al-matrix carbon nanotube composites processed by high pressure torsion of the powders. Journal of Materials Science, 2010, 45, 4652-4658.	1.7	44
72	Grain boundary engineering approach to improve hydrogen embrittlement resistance in Fe Mn C TWIP steel. International Journal of Hydrogen Energy, 2018, 43, 10129-10140.	3.8	44

#	Article	IF	CITATIONS
73	Stress induced crystallization of amorphous materials and mechanical properties of nanocrystalline materials: a molecular dynamics simulation study. Acta Materialia, 2003, 51, 6233-6240.	3.8	42
74	Effect of post-rolling after ECAP on deformation behavior of ECAPed commercial Al–Mg alloy at 723K. Materials Science & Engineering A: Structural Materials: Properties, Microstructure and Processing, 2005, 393, 118-124.	2.6	42
75	Constitutive analysis of the high-temperature deformation mechanisms of Ti–6Al–4V and Ti–6.85Al–1.6V alloys. Materials Science & Engineering A: Structural Materials: Properties, Microstructure and Processing, 2005, 394, 366-375.	2.6	42
76	Effect of heat treatment path on the cold formability of drawn dual-phase steels. Materials Science & Engineering A: Structural Materials: Properties, Microstructure and Processing, 2007, 449-451, 1135-1138.	2.6	42
77	Low-temperature superplasticity and coarsening behavior of Ti–6Al–2Sn–4Zr–2Mo–0.1Si. Materials Science & Engineering A: Structural Materials: Properties, Microstructure and Processing, 2010, 527, 5203-5211.	2.6	42
78	Effect of microstructure on deformation behavior of Ti–6Al–4V alloy during compressing process. Materials & Design, 2012, 36, 796-803.	5.1	42
79	Enhancing impact fracture toughness and tensile properties of a microalloyed cast steel by hot forging and post-forging heat treatment processes. Materials & Design, 2013, 47, 227-233.	5.1	42
80	Role of rolling temperature in the precipitation hardening characteristics of Ti–Mo microalloyed hot-rolled high strength steel. Materials Science & Engineering A: Structural Materials: Properties, Microstructure and Processing, 2014, 615, 255-261.	2.6	42
81	Size and distribution of particles and voids pre-existing in equal channel angular pressed 5083 Al alloy: their effect on cavitation during low-temperature superplastic deformation. Materials Science & Engineering A: Structural Materials: Properties, Microstructure and Processing, 2004, 371, 178-186.	2.6	41
82	Enhancing mechanical properties of a low-carbon microalloyed cast steel by controlled heat treatment. Materials Science & amp; Engineering A: Structural Materials: Properties, Microstructure and Processing, 2013, 559, 427-435.	2.6	41
83	A crystal plasticity model for describing the anisotropic hardening behavior of steel sheets during strain-path changes. International Journal of Plasticity, 2018, 111, 85-106.	4.1	40
84	Effect of W addition on the low cycle fatigue behavior of high Cr ferritic steels. Materials Science & Engineering A: Structural Materials: Properties, Microstructure and Processing, 2001, 298, 127-136.	2.6	39
85	Effect of carbon content on mechanical properties of fully pearlitic steels. Materials Science and Technology, 2002, 18, 1317-1321.	0.8	39
86	A Self-Consistent Approach for Modeling the Flow Behavior of the Alpha and Beta Phases in Ti-6Al-4V. Metallurgical and Materials Transactions A: Physical Metallurgy and Materials Science, 2011, 42, 1805-1814.	1.1	39
87	Low-cycle fatigue properties of CoCrFeMnNi high-entropy alloy compared with its conventional counterparts. Materials Science & Engineering A: Structural Materials: Properties, Microstructure and Processing, 2020, 792, 139661.	2.6	39
88	Role of initial texture on the plastic anisotropy of Mg–3Al–1Zn alloy at various temperatures. Materials Science & Engineering A: Structural Materials: Properties, Microstructure and Processing, 2011, 528, 1162-1172.	2.6	38
89	Increased resistance to hydrogen embrittlement in high-strength steels composed of granular bainite. Materials Science & Engineering A: Structural Materials: Properties, Microstructure and Processing, 2017, 700, 473-480.	2.6	38
90	Effect of interlamellar spacing on the delamination of pearlitic steel wires. Scripta Materialia, 1996, 35, 641-646.	2.6	37

#	Article	IF	CITATIONS
91	Determination of the beta-approach curve and beta-transus temperature for titanium alloys using sensitivity analysis of a trained neural network. Materials Science & Engineering A: Structural Materials: Properties, Microstructure and Processing, 2006, 434, 218-226.	2.6	37
92	High-temperature deformation and grain-boundary characteristics of titanium alloys with an equiaxed microstructure. Materials Science & Engineering A: Structural Materials: Properties, Microstructure and Processing, 2008, 485, 601-612.	2.6	35
93	Microstructure evolution and properties of Mg–3Sn–1Mn (wt%) alloy strip processed by semisolid rheo-rolling. Journal of Materials Processing Technology, 2012, 212, 1430-1436.	3.1	35
94	An Improvement on Prediction of Fatigue Crack Growth from Low Cycle Fatigue Properties. Engineering Fracture Mechanics, 1998, 60, 397-406.	2.0	34
95	Microstructural Mechanisms during Dynamic Globularization of Ti-6Al-4V Alloy. Materials Transactions, 2008, 49, 2196-2200.	0.4	34
96	Enhanced mechanical compatibility of submicrocrystalline Ti–13Nb–13Zr alloy. Materials Science & Engineering A: Structural Materials: Properties, Microstructure and Processing, 2010, 527, 4914-4919.	2.6	34
97	Anisotropic fatigue behavior of rolled Mg–3Al–1Zn alloy. Journal of Materials Research, 2010, 25, 966-971.	1.2	34
98	Role of Mo/V carbides in hydrogen embrittlement of tempered martensitic steel. Corrosion Reviews, 2015, 33, 433-441.	1.0	34
99	Deformation characteristics of submicrocrystalline Ti–6Al–4V. Scripta Materialia, 2008, 58, 1094-1097.	2.6	33
100	Influence of loading direction on the anisotropic fatigue properties of rolled magnesium alloy. International Journal of Fatigue, 2016, 87, 210-215.	2.8	33
101	Effect of V/Mo ratio on the evolution of carbide precipitates and hydrogen embrittlement of tempered martensitic steel. Corrosion Science, 2020, 176, 108929.	3.0	33
102	Nanoscale graphene coating on commercially pure titanium for accelerated bone regeneration. RSC Advances, 2016, 6, 26719-26724.	1.7	32
103	Superplasticity of fine-grained 7475 Al alloy and a proposed new deformation mechanism. Acta Materialia, 1997, 45, 5195-5202.	3.8	31
104	Microstructural evolution and strain-hardening behavior of multi-pass caliber-rolled Ti–13Nb–13Zr. Materials Science & Engineering A: Structural Materials: Properties, Microstructure and Processing, 2015, 648, 359-366.	2.6	31
105	Effects of pre-tension on fatigue behavior of rolled magnesium alloy. Materials Science & Engineering A: Structural Materials: Properties, Microstructure and Processing, 2017, 680, 351-358.	2.6	31
106	Effect of Ce addition on secondary phase transformation and mechanical properties of 27Cr–7Ni hyper duplex stainless steels. Materials Science & Engineering A: Structural Materials: Properties, Microstructure and Processing, 2013, 573, 27-36.	2.6	30
107	Effect of carbon content on the Hall-Petch parameter in cold drawn pearlitic steel wires. Journal of Materials Science, 2002, 37, 2243-2249.	1.7	29
108	Formation of a submicrocrystalline structure in a two-phase titanium alloy without severe plastic deformation. Scripta Materialia, 2013, 68, 996-999.	2.6	29

#	Article	IF	CITATIONS
109	Enhancing high-cycle fatigue properties of cold-drawn Fe–Mn–C TWIP steels. International Journal of Fatigue, 2016, 85, 57-64.	2.8	29
110	Microstructural influence on fatigue properties of a high-strength spring steel. Materials Science & Engineering A: Structural Materials: Properties, Microstructure and Processing, 1998, 241, 30-37.	2.6	28
111	Effects of Sintering Conditions on the Mechanical Properties of Metal Injection Molded 316L Stainless Steel ISIJ International, 2003, 43, 119-126.	0.6	28
112	High Temperature Deformation Behavior of Beta-Gamma TiAl Alloy. Materials Science Forum, 0, 539-543, 1531-1536.	0.3	28
113	Neural network modelling of flow stress in Ti–6Al–4V alloy with equiaxed and Widmanstäten microstructures. Materials Science and Technology, 2008, 24, 294-301.	0.8	28
114	Improved preâ€osteoblast response and mechanical compatibility of ultrafineâ€grained Ti–13Nb–13Zr alloy. Clinical Oral Implants Research, 2011, 22, 735-742.	1.9	28
115	Anisotropic twinning and slip behaviors and their relative activities in rolled alpha-phase titanium. Materials Science & Engineering A: Structural Materials: Properties, Microstructure and Processing, 2017, 698, 54-62.	2.6	28
116	Influence of hydrogen on the grain boundary crack propagation in bcc iron: A molecular dynamics simulation. Computational Materials Science, 2018, 149, 424-434.	1.4	27
117	Dynamic deformation behavior and microstructural evolution during high-speed rolling of Mg alloy having non-basal texture. Journal of Materials Science and Technology, 2019, 35, 473-482.	5.6	27
118	Effect of grain size on the low-cycle fatigue behavior of carbon-containing high-entropy alloys. Materials Science & Engineering A: Structural Materials: Properties, Microstructure and Processing, 2021, 810, 140985.	2.6	27
119	High Temperature Deformation Behavior of Ti-6Al-4V Alloy with an Equiaxed Microstructure: a Neural Networks Analysis. Metals and Materials International, 2008, 14, 213-221.	1.8	26
120	Microstructure prediction of two-phase titanium alloy during hot forging using artificial neural networks and FE simulation. Metals and Materials International, 2009, 15, 427-437.	1.8	26
121	A strain energy-based approach to the low-cycle fatigue damage mechanism in a high-strength spring steel. Metallurgical and Materials Transactions A: Physical Metallurgy and Materials Science, 1998, 29, 1431-1439.	1.1	25
122	Effect of stress state on the high temperature workability of AZ31 Mg alloy. Metals and Materials International, 2010, 16, 197-203.	1.8	25
123	Surface structures and osteoblast response of hydrothermally produced CaTiO3 thin film on Ti–13Nb–13Zr alloy. Applied Surface Science, 2011, 257, 7856-7863.	3.1	25
124	Mechanical and microstructural analysis on the superplastic deformation behavior of Ti–6Al–4V Alloy. International Journal of Mechanical Sciences, 2000, 42, 1555-1569.	3.6	24
125	Enhanced low-cycle fatigue life by pre-straining in an Fe-17Mn-0.8C twinning induced plasticity steel. Metals and Materials International, 2014, 20, 1043-1051.	1.8	24
126	Manufacturing Ultrafine-Grained Ti-6Al-4V Bulk Rod Using Multi-Pass Caliber-Rolling. Metals, 2015, 5, 777-789.	1.0	24

#	Article	IF	CITATIONS
127	Three-dimensional real structure-based finite element analysis of mechanical behavior for porous titanium manufactured by a space holder method. Computational Materials Science, 2015, 100, 2-7.	1.4	24
128	Effect of Al addition on low-cycle fatigue properties of hydrogen-charged high-Mn TWIP steels. Materials Science & Engineering A: Structural Materials: Properties, Microstructure and Processing, 2016, 677, 421-430.	2.6	24
129	Effect of the amount and temperature of prestrain on tensile and low-cycle fatigue properties of Fe-17Mn-0.5C TRIP/TWIP steel. Materials Science & Engineering A: Structural Materials: Properties, Microstructure and Processing, 2017, 696, 493-502.	2.6	24
130	Comparative study on the effects of Cr, V, and Mo carbides for hydrogen-embrittlement resistance of tempered martensitic steel. Scientific Reports, 2019, 9, 5219.	1.6	24
131	Effect of microstructural features on ductility in hypo-eutectoid steels. Scripta Materialia, 1999, 41, 605-610.	2.6	23
132	High-temperature deformation behavior of a gamma TiAl alloy—Microstructural evolution and mechanisms. Metallurgical and Materials Transactions A: Physical Metallurgy and Materials Science, 2003, 34, 2165-2176.	1.1	23
133	Constitutive analysis of compressive deformation behavior of ELI-grade Ti–6Al–4V with different microstructures. Journal of Materials Science, 2012, 47, 3115-3124.	1.7	23
134	Simultaneous Improvement in the Strength and Formability of Commercially Pure Titanium via Twinning-induced Crystallographic Texture Control. Scientific Reports, 2019, 9, 2009.	1.6	23
135	Effect of tempering duration on hydrogen embrittlement of vanadium-added tempered martensitic steel. International Journal of Hydrogen Energy, 2021, 46, 19670-19681.	3.8	23
136	Relationship between mechanical properties and high-cycle fatigue strength of medium-carbon steels. Materials Science & Engineering A: Structural Materials: Properties, Microstructure and Processing, 2017, 690, 185-194.	2.6	22
137	Mechanical properties of Fe–Ni–Cr–Si–B bulk glassy alloy. Materials Science & Engineering A: Structural Materials: Properties, Microstructure and Processing, 2007, 449-451, 181-184.	2.6	21
138	Static and Dynamic Deformation of Fully Austenitic High Mn Steels. Procedia Engineering, 2011, 10, 1002-1006. Enhancing yield strength by suppressing detwinning in a rolled Mga€"3Ala€"1Zn alloy with {cmml:math	1.2	20
139	xmlns:mml="http://www.w3.org/1998/Math/MathML" altimg="si0002.gif" overflow="scroll"> <mml:mn>10</mml:mn> <mml:mover accent="true"><mml:mn>1</mml:mn><mml:mo>Â⁻</mml:mo><mml:mn>2</mml:mn>twins. Materials Science & amp: Engineering A: Structural Materials: Properties. Microstructure and</mml:mover 	> } .6	20
140	Processing, 2014, 619, 328-333. Comparative study of tensile and high-cycle fatigue properties of extruded AZ91 and AZ91–0.3Ca–0.2Y alloys. Journal of Materials Science and Technology, 2021, 93, 41-52.	5.6	20
141	Acoustic Emission Behavior during Tensile Tests of Low Carbon Steel Welds ISIJ International, 1999, 39, 365-370.	0.6	19
142	Internal-variable analysis of high-temperature deformation behavior of Ti–6Al–4V: A comparative study of the strain-rate-jump and load-relaxation tests. Materials Science & Engineering A: Structural Materials: Properties, Microstructure and Processing, 2013, 562, 180-189.	2.6	19
143	Abnormal texture evolution of rolled Mg–3Al–1Zn alloy containing initial {10-12} twins. Scripta Materialia, 2015, 99, 21-24.	2.6	19
144	Prediction of hole expansion ratio for various steel sheets based on uniaxial tensile properties. Metals and Materials International, 2018, 24, 187-194.	1.8	19

#	Article	IF	CITATIONS
145	Grain elongation in a superplastic 7075 Al alloy. Scripta Materialia, 1999, 41, 269-274.	2.6	18
146	Effects of microstructural parameters on the fatigue crack growth of fully lamellar Î ³ -TiAl alloys. Materials Science & Engineering A: Structural Materials: Properties, Microstructure and Processing, 2002, 329-331, 545-556.	2.6	18
147	Analysis of stress states in compression stage of high pressure torsion using slab analysis method and finite element method. Metals and Materials International, 2013, 19, 1021-1027.	1.8	18
148	Fatigue crack propagation in Al-Li 8090 alloy at room (300K) and cryogenic (77K) temperatures. Scripta Materialia, 1996, 34, 215-220.	2.6	17
149	High temperature deformation behavior of a Î ³ TiAl alloy determined using the load-relaxation test. Materials Science & Engineering A: Structural Materials: Properties, Microstructure and Processing, 2003, 344, 146-157.	2.6	17
150	Effects of Temperature and Strain Rate on the High-Temperature Workability of Strip-Cast Mg-3Al-1Zn Alloy. Metallurgical and Materials Transactions A: Physical Metallurgy and Materials Science, 2008, 39, 1426-1434.	1.1	16
151	Effect of Wavelike Sloping Plate Rheocasting on Microstructures of Hypereutectic Al-18Âpct Si-5Âpct Fe Alloys. Metallurgical and Materials Transactions B: Process Metallurgy and Materials Processing Science, 2012, 43, 337-343.	1.0	16
152	Effects of tungsten addition and heat treatment conditions on microstructure and mechanical properties of microalloyed forging steels. Materials Science & Engineering A: Structural Materials: Properties, Microstructure and Processing, 2013, 562, 144-151.	2.6	16
153	Hydrogen Embrittlement Behavior of 430 and 445NF Ferritic Stainless Steels. Metallurgical and Materials Transactions A: Physical Metallurgy and Materials Science, 2013, 44, 1331-1339.	1.1	16
154	Anisotropic in-plane fatigue behavior of rolled magnesium alloy with {10â^'12} twins. Materials Science & Engineering A: Structural Materials: Properties, Microstructure and Processing, 2017, 700, 191-197.	2.6	16
155	Coarsening kinetics of primary alpha in a near alpha titanium alloy. Journal of Alloys and Compounds, 2018, 735, 1769-1777.	2.8	16
156	Superplasticity of V10Cr15Mn5Fe35Co10Ni25 high-entropy alloy processed using high-pressure torsion. Materials Science & Engineering A: Structural Materials: Properties, Microstructure and Processing, 2019, 764, 138198.	2.6	16
157	Acoustic emission measurement of fatigue crack closure. Scripta Metallurgica Et Materialia, 1995, 32, 701-706.	1.0	15
158	Effects of volume fraction of tempered martensite on dynamic deformation properties of a Ti-6Al-4V alloy having a bimodal microstructure. Metallurgical and Materials Transactions A: Physical Metallurgy and Materials Science, 2005, 36, 741-748.	1.1	15
159	High Temperature Deformation Behavior of AZ31 Mg Alloy. Materials Science Forum, 2005, 475-479, 2927-2930.	0.3	15
160	Mechanisms of tensile improvement in caliber-rolled high-carbon steel. Metals and Materials International, 2012, 18, 391-396.	1.8	15
161	Hollow cone high-pressure torsion: Microstructure and tensile strength by unique severe plastic deformation. Scripta Materialia, 2014, 71, 41-44.	2.6	15
162	Phase transformation and its effect on mechanical characteristics in warm-deformed Ti-29Nb-13Ta-4.6Zr alloy. Metals and Materials International, 2015, 21, 202-207.	1.8	15

#	Article	IF	CITATIONS
163	Role of deformation twins in static recrystallization kinetics of high-purity alpha titanium. Metals and Materials International, 2016, 22, 1041-1048.	1.8	15
164	Precise determination of fatigue crack closure in Al alloys. Materials Science & Engineering A: Structural Materials: Properties, Microstructure and Processing, 1996, 216, 131-138.	2.6	14
165	Effect of volume fraction of undissolved cementite on the high cycle fatigue properties of high carbon steels. International Journal of Fatigue, 2007, 29, 1863-1867.	2.8	14
166	Dynamic tensile extrusion behavior of coarse grained and ultrafine grained OFHC Cu. Materials Science & Engineering A: Structural Materials: Properties, Microstructure and Processing, 2013, 569, 61-70.	2.6	14
167	Effects of tungsten on continuous cooling transformation characteristics of microalloyed steels. Materials & Design, 2013, 49, 252-258.	5.1	14
168	Hardness and microstructure of interstitial free steels in the early stage of high-pressure torsion. Journal of Materials Science, 2013, 48, 4698-4704.	1.7	14
169	Effects of carbon content on the tensile and fatigue properties in hydrogen-charged Fe-17Mn-xC steels: The opposing trends. Materials Science & Engineering A: Structural Materials: Properties, Microstructure and Processing, 2018, 724, 469-476.	2.6	14
170	High strain-rate superplasticity of AZ91 alloy achieved by rapidly solidified flaky powder metallurgy. Materials Letters, 2019, 234, 245-248.	1.3	14
171	Effect of ECAP Strain on Deformation Behavior at Low Temperature Superplastic Regime of Ultrafine Grained 5083 Al Alloy Fabricated by ECAP. Materials Transactions, 2004, 45, 958-963.	0.4	13
172	Deformation Behavior of Ti-6Al-4V and Ti-6.85Al-1.6V Alloy with a Globular Microstructure. Materials Science Forum, 2005, 475-479, 2965-2968.	0.3	13
173	A Novel Semisolid Rheo-Rolling Process of AZ31 Alloy with Vibrating Sloping Plate. Materials and Manufacturing Processes, 2013, 28, 299-305.	2.7	13
174	Structure and Stoichiometry of MgxZny in Hot-Dipped Zn–Mg–Al Coating Layer on Interstitial-Free Steel. Metals and Materials International, 2018, 24, 1090-1098.	1.8	13
175	Orientation Dependence on Plastic Flow Behavior of Hydrogen-Precharged Micropillars of High-Mn Steel. Metals and Materials International, 2020, 26, 1741-1748.	1.8	13
176	Tailoring Extra-Strength of a TWIP Steel by Combination of Multi-Pass Equal-Channel Angular Pressing and Warm Rolling. Metals, 2021, 11, 518.	1.0	13
177	Microstructural evolution and mechanical properties of nanocrystalline Fe–Mn–Al–C steel processed by high-pressure torsion. Materials Science & Engineering A: Structural Materials: Properties, Microstructure and Processing, 2021, 827, 142073.	2.6	13
178	Plastic equation of state and load relaxation behavior of pure tin. Scripta Materialia, 1996, 35, 635-640.	2.6	12
179	Effects of microstructural parameters on work hardening of pearlite at small strains. Metallurgical and Materials Transactions A: Physical Metallurgy and Materials Science, 2000, 31, 2665-2669.	1.1	12
180	A microstructural model for predicting high cycle fatigue life of steels. International Journal of Fatigue, 2005, 27, 1115-1123.	2.8	12

#	Article	IF	CITATIONS
181	Effects of Tungsten Addition on the Microstructure and Mechanical Properties of Microalloyed Forging Steels. Metallurgical and Materials Transactions A: Physical Metallurgy and Materials Science, 2013, 44, 3511-3523.	1.1	12
182	Microstructure formation mechanism and properties of AZ61 alloy processed by melt treatment with vibrating cooling slope and semisolid rolling. Metals and Materials International, 2013, 19, 1063-1067.	1.8	12
183	Enhancing low-cycle fatigue life of commercially-pure Ti by deformation at cryogenic temperature. Materials Science & Engineering A: Structural Materials: Properties, Microstructure and Processing, 2021, 803, 140698.	2.6	12
184	Microstructural evolution during superplastic bulge forming of Ti–6Al–4V alloy. Materials Science & Engineering A: Structural Materials: Properties, Microstructure and Processing, 1998, 243, 119-125.	2.6	11
185	Mechanism of Martensitic to Equiaxed Microstructure Evolution during Hot Deformation of a Near-Alpha Ti Alloy. Metallurgical and Materials Transactions A: Physical Metallurgy and Materials Science, 2017, 48, 2979-2992.	1.1	11
186	Hydrogen Embrittlement Behavior of 18Ni 300 Maraging Steel Produced by Selective Laser Melting. Materials, 2019, 12, 2360.	1.3	11
187	Effect of bainite fraction on hydrogen embrittlement of bainite/martensite steel. Materials Science & Engineering A: Structural Materials: Properties, Microstructure and Processing, 2021, 814, 141226.	2.6	11
188	Effect of type-C liquid metal embrittlement on mechanical properties of spot-welded TRIP steel. Journal of Materials Research and Technology, 2021, 13, 2482-2490.	2.6	11
189	Interface characteristics and mechanical behavior of additively manufactured multi-material of stainless steel and Inconel. Materials Science & Engineering A: Structural Materials: Properties, Microstructure and Processing, 2022, 847, 143318.	2.6	11
190	Microstructural influence on the fatigue crack propagation of a Î ³ -TiAl alloy. Scripta Materialia, 1997, 36, 821-827.	2.6	10
191	Mechanical and microstructural analysis on the superplastic deformation behavior of two-phase ti-6a1-4v alloy. Metals and Materials International, 1998, 4, 771-777.	0.2	10
192	An internal variable approach for anomalous yield phenomena of β-CuZn alloy. Acta Materialia, 2004, 52, 2913-2922.	3.8	10
193	Role of nitrogen in the cyclic deformation behavior of duplex stainless steels. Metallurgical and Materials Transactions A: Physical Metallurgy and Materials Science, 2005, 36, 967-976.	1.1	10
194	Superplastic deformation behavior of ultra-fine-grained 5083 Al alloy using load-relaxation tests. Materials Science & Engineering A: Structural Materials: Properties, Microstructure and Processing, 2007, 449-451, 756-760.	2.6	10
195	FATIGUE LIFE PREDICTION OF ROLLED AZ31 MAGNESIUM ALLOY USING AN ENERGY-BASED MODEL. International Journal of Modern Physics B, 2008, 22, 5503-5508.	1.0	10
196	Factors Influencing Tensile Ductility of OFHC Cu Having Different Ultrafine Grained Structures. Materials Transactions, 2010, 51, 2049-2055.	0.4	10
197	Effect of the casting temperature on temperature field and microstructure of A2017 alloy during an innovative continuous semisolid rolling process with a vibrating sloping plate device. International Journal of Advanced Manufacturing Technology, 2013, 67, 917-923.	1.5	10
198	Microstructure and properties of Mg–3Sn–1Mn (wt%) alloy processed by a novel continuous shearing and rolling and heat treatment. Materials Science & Engineering A: Structural Materials: Properties, Microstructure and Processing, 2013, 559, 194-200.	2.6	10

#	Article	IF	CITATIONS
199	Effect of Intergranular Ferrite on Hydrogen Delayed Fracture Resistance of Ultrahigh Strength Boron-added Steel. ISIJ International, 2007, 47, 913-919.	0.6	10
200	Origin of superior low-cycle fatigue resistance of an interstitial metastable high-entropy alloy. Journal of Materials Science and Technology, 2022, 115, 115-128.	5.6	10
201	Reverse Austenite Transformation Behavior of Equal Channel Angular Pressed Low Carbon Ferrite/Pearlite Steel. ISIJ International, 2007, 47, 294-298.	0.6	9
202	Effect of tungsten addition on the mechanical properties and corrosion resistance of S355NL forging steel. Metals and Materials International, 2012, 18, 217-223.	1.8	9
203	Effect ofl ² volume fraction on the dynamic grain growth during superplastic deformation of Ti3Al-based alloys. Metals and Materials International, 1998, 4, 1041-1046.	0.2	8
204	A unified constitutive model for quasi-static flow responses of pure Ta and Ta–W alloys. Materials Science & Engineering A: Structural Materials: Properties, Microstructure and Processing, 2011, 528, 1154-1161.	2.6	8
205	Microstructure formation mechanism and properties of a Mg-3Sn-1Mn (wt%) magnesium alloy processed by a novel semisolid continuous shearing and rolling process. Metals and Materials International, 2013, 19, 33-38.	1.8	8
206	Microstructural Influence on Stretch Flangeability of Ferrite–Martensite Dual-Phase Steels. Crystals, 2020, 10, 1022.	1.0	8
207	Effect of undissolved Nb carbides on mechanical properties of hydrogen-precharged tempered martensitic steel. Scientific Reports, 2020, 10, 11704.	1.6	8
208	Influence of Microstructure on Low-Cycle and Extremely-Low-Cycle Fatigue Resistance of Low-Carbon Steels. Metals and Materials International, 2021, 27, 3862-3874.	1.8	8
209	Constitutive analysis on superplastic deformation mechanisms of two-phase Ti3Al–xNb alloy. Materials Science & Engineering A: Structural Materials: Properties, Microstructure and Processing, 2005, 394, 117-125.	2.6	7
210	High-Temperature Deformation Behavior of ELI Grade Ti-6Al-4V Alloy with Martensite Microstructure. Materials Science Forum, 2007, 551-552, 365-372.	0.3	7
211	Factors influencing the equal-channel angular pressing of Ti–6Al–4V alloy having lamellar microstructure. Materials Science & Engineering A: Structural Materials: Properties, Microstructure and Processing, 2008, 493, 164-169.	2.6	7
212	High-cycle fatigue characteristics of non-heat-treated steels developed for bolt applications. Materials Science & Engineering A: Structural Materials: Properties, Microstructure and Processing, 2012, 550, 118-124.	2.6	7
213	Enhancing Superplasticity of Ultrafineâ€Grained Ti–6Al–4V without Imposing Severe Plastic Deformation. Advanced Engineering Materials, 2019, 21, 1800115.	1.6	7
214	Improved cold-rollability of duplex lightweight steels utilizing deformation-induced ferritic transformation. Materials Science & Engineering A: Structural Materials: Properties, Microstructure and Processing, 2019, 742, 835-841.	2.6	7
215	Microstructural influence on the intrinsic fatigue properties of Alî—,Li 8090 alloy. Materials Science & Engineering A: Structural Materials: Properties, Microstructure and Processing, 1995, 190, 99-108.	2.6	6
216	Effects of microstructure and specimen thickness on the fatigue crack closure in Al-Li 8090 alloy. Scripta Metallurgica Et Materialia, 1995, 32, 1119-1124.	1.0	6

#	Article	IF	CITATIONS
217	Predicting the Adiabatic Temperature of Transparent Y ₃ Al ₅ O ₁₂ Prepared via Combustion Synthesis under Ultra-High Gravity. Materials Transactions, 2010, 51, 2230-2235.	0.4	6
218	Tensile failure of 4130 steel having different ultrafine grained structures. Materials Science & Engineering A: Structural Materials: Properties, Microstructure and Processing, 2010, 527, 645-651.	2.6	6
219	FE Analysis of Microstructure Evolution during Ring Rolling Process of a Large-Scale Ti-6Al-4V Alloy Ring. Materials Science Forum, 0, 638-642, 223-228.	0.3	6
220	Temperature distribution and its influence on microstructure of alloy AZ31 during semisolid rheo-rolling process. International Journal of Cast Metals Research, 2013, 26, 247-254.	0.5	6
221	Integrated constitutive model for flow behavior of pure Titanium considering interstitial solute concentration. Metals and Materials International, 2014, 20, 1017-1025.	1.8	6
222	Tribological and corrosion behaviors of warm- and hot-rolled Ti-13Nb-13Zr alloys in simulated body fluid conditions. International Journal of Nanomedicine, 2015, 10 Suppl 1, 207.	3.3	6
223	Effect of Si and Ce Addition on the Microstructure and Pitting Corrosion Resistance of Hyper-Duplex Stainless Steels. Corrosion, 2015, 71, 470-482.	0.5	6
224	Comparison of Cold Formability of Cold Drawn Non-heat-treated Steels Having Similar Strength. ISIJ International, 2005, 45, 1352-1357.	0.6	6
225	Effect of Texture and {10-12} Twin on the Low Cycle Fatigue Properties of Rolled AZ31 Mg Alloy. Journal of Korean Institute of Metals and Materials, 2013, 51, 325-332.	0.4	6
226	The effect of strain rate on the anomalous peak of yield stress in β-CuZn alloy. Scripta Materialia, 1998, 39, 1289-1294.	2.6	5
227	Quantitative elemental analysis of FeZn-alloy coating by nondestructive method. X-Ray Spectrometry, 2008, 37, 561-564.	0.9	5
228	Characterization of Deformation Behaviors and Elastic Moduli of Multilayered Films in Piezoelectric Inkjet Head. Journal of Microelectromechanical Systems, 2008, 17, 1155-1163.	1.7	5
229	The role of ultrasonic nanocrystalline surface modification at elevated temperature on the hydrogen charging behavior of high-Mn steels. Materialia, 2020, 9, 100626.	1.3	5
230	Effects of W Addition and Heat-treatment on Corrosion Fatigue Crack Growth Behavior of Duplex Stainless Steels ISIJ International, 1997, 37, 1146-1152.	0.6	4
231	Improvement of sag resistance by the addition of tungsten in SiCrMoV steels. Scripta Materialia, 1997, 36, 1315-1320.	2.6	4
232	Ultra-high-speed exploding properties of Ti-6Al-4V alloy having equiaxed and bimodal microstructures. Metallurgical and Materials Transactions A: Physical Metallurgy and Materials Science, 2004, 35, 719-724.	1.1	4
233	Analysis on dynamic tensile extrusion behavior of UFG OFHC Cu. IOP Conference Series: Materials Science and Engineering, 2014, 63, 012144.	0.3	4
234	Effects of dynamic recrystallisation during deep rolling of semisolid slab and heat treatment on microstructure and properties of AZ31 alloy. Materials Science and Technology, 2014, 30, 309-315.	0.8	4

#	Article	IF	CITATIONS
235	Recent Development in Micromanufacturing of Metallic Materials. Materials, 2020, 13, 4046.	1.3	4
236	Ambivalent Role of Annealing in Tensile Properties of Step-Rolled Ti-6Al-4V with Ultrafine-Grained Structure. Metals, 2020, 10, 684.	1.0	4
237	High Temperature Deformation Behavior and Microstructure Evolution of Ti-4Al-4Fe-0.25Si Alloy. Journal of Korean Institute of Metals and Materials, 2016, 54, 338-346.	0.4	4
238	Effects of temperature on the fatigue crack growth of an Al-Li 8090 alloy with δ' microstructure. Metallurgical and Materials Transactions A: Physical Metallurgy and Materials Science, 1997, 28, 1089-1093.	1.1	3
239	Fatigue Crack Propagation Behavior of AZ91D Magnesium Alloy. Materials Science Forum, 2003, 419-422, 75-80.	0.3	3
240	Prediction of Microstructure During High Temperature Forming of Ti-6Al-4V Alloy. Materials Science Forum, 2004, 449-452, 189-192.	0.3	3
241	Superplastic Deformation of Ultrafine Grained Al Alloy Processed by ECAP and Post-Rolling. Materials Science Forum, 2006, 503-504, 119-124.	0.3	3
242	Ring-Rolling Process for Manufacturing Ti-6Al-4V Plane and Profiled Ring-Products. Advanced Materials Research, 2007, 26-28, 429-432.	0.3	3
243	Characterization of Dynamic Globularization Behavior during Hot Working of Ti-6Al-4V Alloy. Advanced Materials Research, 2007, 26-28, 1033-1036.	0.3	3
244	Process Design of Profile Ring Rolling for Turbine Diaphragm Using FEM Simulation. Key Engineering Materials, 2007, 345-346, 1557-1560.	0.4	3
245	An Improved Process Design for the Hot Backward Extrusion of Ti-6Al-4V Tubes Using a Finite Element Method and Continuum Instability Criterion. Proceedings of the Institution of Mechanical Engineers, Part B: Journal of Engineering Manufacture, 2007, 221, 255-265.	1.5	3
246	Hydrogen Embrittlement of Low Carbon HSLA Steel during Slow Strain Rate Test. Advanced Materials Research, 0, 197-198, 642-645.	0.3	3
247	Effects of process parameters on microstructure and properties of AZ91 alloy prepared by cooling/stirring and rolling process. International Journal of Cast Metals Research, 2012, 25, 225-231.	0.5	3
248	Boundary layer and cooling rate and microstructure formation on the cooling sloping plate. Metals and Materials International, 2013, 19, 949-957.	1.8	3
249	Dislocation structure associated with deformation behavior of Fe3Al alloys. Scripta Materialia, 1996, 35, 1041-1046.	2.6	2
250	Acoustic emission characteristics associated with microstructures and plate orientations of an AlLi 8090 alloy. Materials Science & Engineering A: Structural Materials: Properties, Microstructure and Processing, 1997, 229, 219-227.	2.6	2
251	High Temperature Forming of Ti-6Al-4V Alloy Considering Microstructural Evolution. Key Engineering Materials, 2004, 274-276, 117-122.	0.4	2
252	Load Relaxation Behavior of Ultra-Fine Grained Ti-6Al-4V Alloy. Materials Science Forum, 2005, 475-479, 2955-2960.	0.3	2

#	Article	IF	CITATIONS
253	Superplastic Behavior of As-Equal Channel Angular Pressed 5083 Al and 5083 Al-0.2 Sc Alloys. Materials Science Forum, 2005, 475-479, 2937-2940.	0.3	2
254	Reappraisal of grain boundary diffusion creep equations for nanocrystalline materials. Metals and Materials International, 2006, 12, 107-113.	1.8	2
255	Continuum Damage Model of Creep-Fatigue Interaction in Ni-Base Superalloy. Key Engineering Materials, 2007, 340-341, 235-240.	0.4	2
256	Effect of Texture on High Temperature Deformation Behaviors of Ti-6Al-4V Alloy. Key Engineering Materials, 2007, 340-341, 835-840.	0.4	2
257	Investigation of Flow Instability in High Temperature Deformation of INCONEL Alloy 783 Using Processing Map Approach. Key Engineering Materials, 0, 385-387, 501-504.	0.4	2
258	INFLUENCE OF INITIAL MICROSTRUCTURE ON HOT WORKABILITY OF Ti -6 Al -4 V ALLOY. International Journal of Modern Physics B, 2009, 23, 808-813.	1.0	2
259	Evaluation methods for the hoop strength of small-sized tubular ceramic components. Journal of Materials Research, 2009, 24, 1422-1434.	1.2	2
260	Cavitation damage incorporating cavity growth in submicrometer-grained titanium alloy. Journal of Materials Research, 2009, 24, 2161-2165.	1.2	2
261	Prediction of Microstructure Evolution in Hot Backward Extrusion of Ti-6Al-4V Alloy. Journal of Metallurgy, 2012, 2012, 1-6.	1.1	2
262	Microstructure evolution during novel rheorolling process for producing A356 alloy strip. Materials Science and Technology, 2013, 29, 587-593.	0.8	2
263	Effects of deformation parameters on formation of pro-eutectoid cementite in hypereutectoid steels. Journal of Central South University, 2014, 21, 1256-1263.	1.2	2
264	Superior bonding properties of dissimilar steel joint produced by electroslag remelting. Metals and Materials International, 2015, 21, 1054-1060.	1.8	2
265	Effects of drawing strain and post-annealing conditions on microstructural evolution and tensile properties of medium- and high-carbon steels. Metals and Materials International, 2017, 23, 1176-1187.	1.8	2
266	Graded Grain Structure to Improve Hydrogen-Embrittlement Resistance of TWIP Steel. Crystals, 2020, 10, 1045.	1.0	2
267	Effect of Type-B liquid metal embrittlement cracks on high-cycle fatigue properties of spot-welded 1180 TRIP steel. Science and Technology of Welding and Joining, 2021, 26, 173-179.	1.5	2
268	Enhanced Resistance to Delayed Cracking in Deep-drawn Lean Duplex Stainless Steel: the Role of Residual Stress. Journal of Korean Institute of Metals and Materials, 2017, 55, .	0.4	2
269	Effects of morphology and volume fraction of α 2 phase on the fatigue crack propagation of a Ti-24Al-11Nb alloy. Metallurgical and Materials Transactions A: Physical Metallurgy and Materials Science, 1997, 28, 2527-2536.	1.1	1
270	Microstructural influence on sag resistance of Cr containing and Cr free spring steels. Materials Science and Technology, 1998, 14, 827-831.	0.8	1

#	Article	IF	CITATIONS
271	Measurement of Alloying Degree of Galvannealed Steels by X-Ray Diffraction. Key Engineering Materials, 2006, 321-323, 1461-1464.	0.4	1
272	Constitutive Analysis of the High-Temperature Deformation Behavior of Single Phase α-Ti and α+β Ti-6Al-4V Alloy. Materials Science Forum, 2007, 539-543, 3607-3612.	0.3	1
273	Superplastic Behavior of Ultrafine Grained Al Alloys Fabricated by Severe Plastic Deformation. Key Engineering Materials, 2007, 345-346, 597-600.	0.4	1
274	Effect of Heat Treatment on Mechanical Properties of Super Duplex Stainless Steel. Advanced Materials Research, 0, 89-91, 290-294.	0.3	1
275	Microstructural Aspects during the Preparation of Y ₃ Al ₅ O ₁₂ by Combustion Synthesis and Temperature Field Simulation. Materials Transactions, 2011, 52, 685-690.	0.4	1
276	Microstructure and deformation behavior of Ti-10V-2Fe-3Al alloy during hot forming process. Journal Wuhan University of Technology, Materials Science Edition, 2015, 30, 1332-1337.	0.4	1
277	Multicriteria Adaptive Observers for Singular Systems with Unknown Time-Varying Parameters. Mathematical Problems in Engineering, 2017, 2017, 1-10.	0.6	1
278	Constitutive Analysis of the Anisotropic Flow Behavior of Commercially Pure Titanium. Applied Sciences (Switzerland), 2020, 10, 7962.	1.3	1
279	Research Progress of Advanced Titanium Alloys in Korea. Materials Technology, 1998, 5, 331-339.	0.3	0
280	Effect of W-addition on low cycle fatigue behavior of high Cr ferritic steels. Metals and Materials International, 1999, 5, 559-562.	0.2	0
281	High Temperature Deformation Behavior of Ti-6Al-4V Alloy with WidmanstÃ e n Microstructure. Materials Science Forum, 2003, 426-432, 689-694.	0.3	0
282	Effects of Pressing Temperature and Initial Microstructure on the Equal Channel Angular Pressing of Ti-6Al-4V Alloy. Key Engineering Materials, 2003, 233-236, 579-584.	0.4	0
283	Yield Stress Anomalous Behavior in β-CuZn Alloy. Materials Science Forum, 2004, 449-452, 841-844.	0.3	0
284	Effects of volume fraction of tempered martensite on dynamic deformation properties of a Ti-6Al-4V alloy having a bimodal microstructure. Metallurgical and Materials Transactions A: Physical Metallurgy and Materials Science, 2005, 36, 741-748.	1.1	0
285	On the Low Strain Rate Regime of Structural Superplasticity - an Internal Variable Approach. Materials Science Forum, 2005, 475-479, 3007-3012.	0.3	0
286	High Temperature Deformation Behavior of Strip-Cast AZ31 Mg Alloy. Advanced Materials Research, 2006, 15-17, 461-466.	0.3	0
287	Cavitation Behavior of Ultra-Fine Grained Ti-6Al-4V Alloy Produced by Equal-Channel Angular Pressing. Materials Science Forum, 2007, 551-552, 621-626.	0.3	0
288	Influence of Initial Texture on Twin Formation and Plastic Deformation of Rolled AZ31 Mg Alloy. Advanced Materials Research, 2007, 26-28, 149-152.	0.3	0

#	Article	IF	CITATIONS
289	Characterization of the interface heat transfer coefficient during non-isothermal bulk forming of Ti–6Al–4 V alloy. Proceedings of the Institution of Mechanical Engineers, Part B: Journal of Engineering Manufacture, 2011, 225, 1703-1712.	1.5	0
290	Process Design Strategies for Producing Heavy Section Steel with Improved Quality. Advanced Materials Research, 0, 652-654, 988-991.	0.3	0
291	FATIGUE LIFE PREDICTION OF ROLLED AZ31 MAGNESIUM ALLOY USING AN ENERGY-BASED MODEL. , 2009, , .		0
292	SIMS investigation of internal hydrogen behavior of TWIP steel. Journal of Surface Analysis (Online), 2019, 26, 142-143.	0.1	0